Fluid Antenna System—Part I: Preliminaries

Kai-Kit Wong, *Fellow, IEEE,* Wee Kiat New, *Member, IEEE,* Xu Hao, *Member, IEEE,* Kin-Fai Tong, *Fellow, IEEE,* and Chan-Byoung Chae, *Fellow, IEEE*

***Abstract*—With research efforts gearing up to build the sixth-generation (6G) mobile communications, it is only logical to seek new mobile technologies that can provide the next generational leap for much better performance under harsher environments. To this end, one interesting concept is fluid antenna system (FAS) which utilizes flexible antenna architectures such as liquid-based antennas, reconfigurable RF pixel-based antennas, stepper motor-based antennas, and etc., to enable reconfigurability of antenna's position (i.e., port). In so doing, tremendous space diversity can be obtained in a novel way. The possibility of accessing seemingly a continuous fading envelope in the spatial domain also means that multiple access can be realized in a simple manner without complex optimization and processing. This is the first of a three-part letter that reviews the basic principles of FAS. Our scope focuses on the physical-layer performance metrics and we discuss the evolution of the channel models being adopted for FAS and summarize the key results highlighting its potential.**

***Index Terms*—6G, Fluid antenna system, Massive connectivity, Multiple access, Wireless communications.**

I. INTRODUCTION

A. Background

IN MOBILE communications, every decade a new generation is born to reach a new height. In the fifth generation (5G), enhancing quality of experience and driving digitalization of industries are the major highlights [1]. Together with the rapid growth of artificial intelligence (AI) and big data, 5G aims to enable connection of everything everywhere. Looking ahead, discussion about the next generation (a.k.a. the sixth generation (6G)) has already begun and the new frontiers have been speculated in several visionary papers, e.g., [2].

More concretely, the industries have published white papers to outline the requirements and use cases of 6G, e.g., [3]–[5]. Some eye-catching targets include extreme high capacity, from $10\mathrm{Gbps}$ in 5G to $1\mathrm{Tbps}$ in 6G, extreme high reliability, from 99.999% in 5G to 99.99999% in 6G, and extreme massive connectivity, from 10^6 $\mathrm{devices/km}^2$ in 5G to 10^7 $\mathrm{devices/km}^2$ in 6G. According to NTT Docomo [3], new use cases for 6G represent some combinations of extreme requirements of the three key 5G use cases, namely enhanced mobile broadband (eMBB), massive machine-type communication (mMTC) and ultra reliable and low latency communication (URLLC).

From [6], [7], it is suggested that the wireless air interface for 6G is going to be relied upon ultra-massive multiple-input multiple-output (MIMO) system [8] which will be supported by the emerging reconfigurable intelligent surface (RIS) technology, a.k.a. intelligent reflecting surface (IRS) [9]. Visible light communications [10] and Terahertz communications [11] will also play an important role to deliver greater capacity by moving up the frequency band for more bandwidth.

It is no wonder that MIMO is dominating the physical layer again. While MIMO transmits signals from active antennas, RIS/IRS reflects signals using passive elements, like a passive beamformer[1] [12]. The fact that MIMO creates capacity out from space without the need of any bandwidth expansion nor increase in transmit power, is extraordinary and makes it an ageless technology. But is it good enough to keep increasing the number of antennas at the base station (BS) and user equipment (UE) to meet our increasing demands?

Despite its brilliance, MIMO, or more accurately multiuser MIMO, is not a simple solution, not in terms of the overhead for acquiring the channel state information (CSI) to be known at the BS and not the complexity for obtaining the precoding matrix. Although massive MIMO promises to be theoretically simple [14], in 5G, a more complex codebook-based precoding design that uses quantized CSI feedback is adopted [15]. Even if the overhead and complexity can be afforded, the Type II 5G New Radio (NR) multiuser MIMO precoding is not easily upgradable to support more users than it is designed to without another standardization effort. There is also the non-orthogonal multiple access (NOMA) technology [16] that many advocate as the solution for massive connectivity. While NOMA is not included in 5G, the strong interest around the world does seem to suggest that NOMA might play a part in 6G. Nevertheless, NOMA is often criticized for the heavy complexity imposing on the UE for interference cancellation, in addition to the need for CSI acquisition, power allocation and user clustering at the BS. Serving more than 3 users in NOMA is unthinkable.

Surely, MIMO will continue to be the core technology but it is fitting to doubt if MIMO alone can cope with the ever-rising demands, especially mMTC due to scalability issues.

B. Be Water, My Friend to Liberate MIMO

Achieving the diversity and multiplexing gains similar to or better than MIMO but without the issues of CSI acquisition and precoding optimization at the BS would have been ideal. Recently, it was suggested in [17], [18] that this might actually be possible using the emerging fluid antenna technology. Fluid antenna refers to any software-controllable fluidic, conductive, dielectric structure, or even reconfigurable RF-pixels that can change its shape and position to reconfigure the gain, radiation pattern, operating frequency, and other characteristics [17]. A famous quote by Bruce Lee, '*Be Water, My Friend*', describes metaphorically what a fluid antenna system (FAS) may represent to achieve ultimate agility for diversity and multiplexing benefits never possible before in mobile communications.

The work is supported in part by the Engineering and Physical Sciences Research Council (EPSRC) under Grant EP/W026813/1. For the purpose of open access, the authors will apply a Creative Commons Attribution (CC BY) licence to any Author Accepted Manuscript version arising.

K. K. Wong, W. K. New, X. Hao and K. F. Tong are with the Department of Electronic and Electrical Engineering, University College London, Torrington Place, United Kingdom. *Corresponding author:* kai-kit.wong@ucl.ac.uk.

K. K. Wong and C. B. Chae are with Yonsei Frontier Laboratory and School of Integrated Technology, Yonsei University, Seoul, 03722, Korea.

[1]Recent research in fact also considered the use of active radiating elements on RIS, so RIS is becoming increasingly similar to MIMO [13].

The concept of FAS is motivated by the recent advances in flexible antennas which may come in the form of liquid-based antennas [19], reconfigurable pixel-based antennas [20], [21], and stepper motor-based antennas [22], [23]. Other forms of flexible antenna structures using, e.g., metamaterials [24], are also possible. Some common types of fluid antenna relevant for mobile communications are discussed in [17]. The future of FAS as a feasible technology seems to be bright.

Indeed FAS presents an exciting new direction to complement and even surpass MIMO. Specifically, recent efforts in FAS consider the possibility of a position-switchable antenna at UE for enhancing the performance of wireless communications systems. In [25], Wong *et al.* first studied such FAS and derived how the size and resolution of fluid antenna impacted the outage probability of a single-user, point-to-point system. Later in [26], closed-form expressions for the level crossing rate of such FAS were developed. Analysis that extended to Nakagami fading channels was given in [27]. Recently, [28] studied FAS to improve Terahertz communications, modelled using the α-μ distribution. The study even considered activating multiple ports of a fluid antenna and performed combining of multi-port signals to further enhance performance. In [29], Khammassi *et al.* proposed jointly correlated channel models to more accurately account for the spatial correlation between the ports of FAS in the performance analysis. Most recently, [30] adopted the channel model in [29] to investigate the diversity order of FAS. Channel estimation and low-complexity port selection for FAS was also studied in [31]. Independently, [32] proposed a movable antenna system, a special case of FAS ignoring the spatial correlation between the ports.

FAS and MIMO can combine to further improve the system performance, leading to the concept of MIMO-FAS[2] in which multiple single-port fluid antennas or multi-port fluid antenna are employed at both ends of the communication channel [33]. FAS offers an additional degree of freedom (DoF) to liberate MIMO for more spatial diversity. In [34], MIMO with movable antennas was studied in deterministic channels ignoring spatial correlation between the antennas. Recently, the information-theoretic performance of MIMO-FAS was investigated in [35], showing that MIMO-FAS outperforms traditional MIMO.

FAS can also be effective for multiuser communications. By shifting the antenna's position (or port) at UE, the UE will be able to access the ups and downs of its interference signal in the spatial domain. In the interest of multiple access, the UE can choose the port where some form of signal-to-interference plus noise ratio (SINR) is maximized. This approach does not need precoding at the BS as in multiuser MIMO nor multiuser detection at the UE like NOMA. All the UE needs to do is to find and activate the best port for reception and the interference signal will disappear naturally due to fading. This technique is referred to as fluid antenna multiple access (FAMA).

In [36], [37], fast FAMA was proposed while [38] studied slow FAMA. The main difference is that fast FAMA switches the antenna port on a per-symbol basis whereas slow FAMA switches only when the channel changes. Under typical situations, it was illustrated that fast FAMA could support tens of UEs whereas slow FAMA could also cope with several UEs on the same radio channel without CSI at the BS nor interference cancellation receivers at the UEs. Opportunistic scheduling in FAMA networks was also recently studied in [39].

C. Aim of This Letter

The aim of this letter is to review some fundamentals of FAS. This is the first of a three-part letter. The second part will discuss research opportunities while the last part will present a new paradigm of combining FAS and RIS.

II. Fluid Antenna, FAS and FAMA

Fluid antenna may take many forms and can possess different reconfigurabilities, depending upon the applications [17]. In this letter, we focus on the position-switchable antenna. In the one-dimensional (1D) FAS case, a fluid antenna has a line structure of size $W\lambda$ with N evenly distributed ports in which λ is the wavelength. Each port represents a physical location to which the radiating element of the antenna can be switched. Port switching can have delay but is often assumed negligible.

For a point-to-point FAS where the transmitter uses a fixed antenna but the receiver has a fluid antenna (i.e., the single-input multiple-output (SIMO) case), the received signal at the k-th port of fluid antenna is given by

$$r_k = g_k s + \eta_k, \tag{1}$$

where g_k denotes the complex channel coefficient at the k-th port, s is the information-bearing symbol and $\eta_k \sim \mathcal{CN}(0,\sigma_\eta^2)$ is the additive white Gaussian noise (AWGN). The channels $\{g_k\}$ are strongly correlated and their model will be discussed.

To optimize the performance, FAS activates the port which has the strongest channel, and has the outage probability

$$p_{\rm FAS} = {\rm Prob}\left(\frac{\sigma_s^2}{\sigma_\eta^2}\max_k\{|g_k|^2\} < \gamma\right), \tag{2}$$

in which $\sigma_s^2 = {\rm E}[|s|^2]$ is the symbol power and γ represents the signal-to-noise ratio (SNR) threshold.

For multiple access, the system (1) can be extended to

$$r_k^{(u)} = g_k^{(u,u)} s_u + \underbrace{\sum_{\substack{\tilde{u}\neq u\\ \tilde{u}=1}}^{U} g_k^{(\tilde{u},u)} s_{\tilde{u}} + \eta_k^{(u)}}_{\tilde{g}_k^{(u)}}, \tag{3}$$

where $r_k^{(u)}$ denotes the received signal at the k-th port of UE u, $g_k^{(\tilde{u},u)}$ denotes the channel from UE $\tilde{u}$'s transmit antenna to the k-th port of UE u's receive antenna, U is the number of UEs occupying the same time-frequency channel and all other variables are defined similarly as in (1) before. The model (3) is valid for interference channels and even broadcast channels if each BS antenna is assigned to transmit one UE's signal.[3]

[2]In [17], MIMO-FAS is referred to as fluid MIMO or flexible MIMO.

[3]The FAMA approach basically treats the downlink channel as an interference channel because the BS antennas operate independently. In that sense, the uplink channel is no different to the downlink channel if FAMA is applied. However, it is worth pointing out that for downlink, getting CSI at the BS for precoding is challenging and FAMA is well placed to simplify the processing. By contrast, in the uplink, it is relatively straightforward to acquire the CSI at the BS to combine the received signals or perform joint decoding.

In slow FAMA [38], each UE activates the port that maximizes the average SINR and it has the outage probability

$$p_{\text{s-FAMA}}=\mathrm{E}\left[\text{Prob}\left(\max_k \frac{\sigma_s^2|g_k^{(u,u)}|^2}{\sigma_s^2\sum_{\substack{\tilde{u}\neq u\\ \tilde{u}=1}}^{U}|g_k^{(\tilde{u},u)}|^2+\sigma_\eta^2}<\gamma\right)\right], \tag{4}$$

where it has been assumed that all UEs have the same symbol energy and γ now denotes the SINR threshold.

For fast FAMA [36], [37], each UE chooses the port that maximizes the ratio between the instantaneous desired signal energy and the instantaneous energy of the sum-interference and noise. Therefore, it has the outage probability

$$p_{\text{f-FAMA}}=\mathrm{E}\left[\text{Prob}\left(\max_k \frac{|g_k^{(u,u)}s_u|^2}{|\tilde{g}_k^{(u)}|^2}<\gamma\right)\right]. \tag{5}$$

Note that with $U=2$, slow FAMA and fast FAMA become identical if the additive noise is ignored or $\sigma_\eta^2\approx 0$.

III. Channel Model

A. SIMO with 1D FAS

The performance of FAS depends strongly on the size W and resolution N of the fluid antenna at the UE because the channels $\{g_k\}$ are correlated to each other as the ports can be very closely located to one another. Characterizing the spatial correlation amongst the ports accurately is an important issue. In the earlier work, e.g., [25]–[28], [36], g_k is modelled as

$$g_k=\sigma\left(\mu_k x_0+\sqrt{1-\mu_k^2}x_k\right)+j\sigma\left(\mu_k y_0+\sqrt{1-\mu_k^2}y_k\right),\ k=1,\dots,N, \tag{6}$$

where $x_0,\dots,x_N,y_0,\dots,y_N\sim\mathcal{N}(0,0.5)$ are independently and identically distributed (i.i.d.), $\mathrm{E}[|g_k|^2]=\sigma^2$ and

$$\mu_k=J_0\left(\frac{2\pi(k-1)}{N-1}W\right), \tag{7}$$

where $J_0(\cdot)$ denotes the zero-order Bessel function of the first kind. The choice in (7) is intended to account for the channel correlation between any two ports due to their distance to each other. However, the limitation of (6) was explained in [40] and it was proposed to set $\mu_k=\mu\ \forall k$ instead and choose

$$\mu=\sqrt{2}\sqrt{{}_1F_2\left(\frac{1}{2};1,\frac{3}{2};-\pi^2W^2\right)-\frac{J_1(2\pi W)}{2\pi W}}, \tag{8}$$

where ${}_aF_b(\cdot;\cdot;\cdot)$ denotes the generalized hypergeometric function and $J_1(\cdot)$ is the first-order Bessel function of the first kind. Setting (8) ensures the model have the same mean correlation coefficient for an N-port line structure of length $W\lambda$. The new model has recently been adopted in [38], [39].

The most accurate analytical model for FAS so far, nonetheless, appears to be the eigenvalue-based model in [29], which was recently used in [30], [35], [41]. In this model, we have

$$g_k=\sigma\sum_{m=1}^{N}\sqrt{\lambda_m}u_{k,m}(x_k+jy_k), \tag{9}$$

in which λ_m and $u_{k,m}$ denote, respectively, the eigenvalue and the entry of the eigenvector matrix of the covariance matrix $\mathrm{E}[\mathbf{g}\mathbf{g}^\dagger]=\sigma^2\mathbf{\Sigma}$ where $\mathbf{g}=[g_1\cdots g_N]^T$. That is, $\mathbf{\Sigma}=\mathbf{U}\mathbf{\Lambda}\mathbf{U}^\dagger$ where $\mathbf{\Lambda}=\text{diag}(\lambda_1,\dots,\lambda_N)$ and $[\mathbf{U}]_{k,m}=u_{k,m}$. To model the spatial correlation among the ports, we have [35]

$$[\mathbf{\Sigma}]_{k,\ell}=\frac{1}{\sigma}\text{Cov}(g_k,g_\ell)=J_0\left(\frac{2\pi(k-\ell)}{N-1}W\right). \tag{10}$$

In [29], it was further shown that $\mathbf{\Sigma}$ is a Hermitian Toeplitz matrix and most importantly, its energy is mainly focused on a few largest eigenvalues. This makes it possible to approximate g_k by considering only $L\le N$ eigenvalues so that

$$g_k\approx\sigma\sum_{m=1}^{L}\sqrt{\lambda_m}u_{k,m}(x_k+jy_k). \tag{11}$$

The model in [29] certainly is most accurate but challenging in performance analysis while the channel model in [40] may be preferred for its tractability but compromise the accuracy.

B. MIMO with 2D FAS

It is also possible to consider a two-dimensional (2D) fluid antenna surface, as opposed to a line structure. Such extension was conducted in [35]. Moreover, fluid antenna can be adopted at both the transmitter and receiver side. In the 2D MIMO-FAS case, the complex channel can be modelled as

$$\mathbf{H}=\mathbf{U}_{\mathrm{R}}\sqrt{\mathbf{\Lambda}_{\mathrm{R}}}\mathbf{G}\sqrt{\mathbf{\Lambda}_{\mathrm{T}}^\dagger}\mathbf{U}_{\mathrm{T}}^\dagger, \tag{12}$$

in which $\mathbf{U}_{\mathrm{T}}$, $\mathbf{\Lambda}_{\mathrm{T}}$, $\mathbf{U}_{\mathrm{R}}$, $\mathbf{\Lambda}_{\mathrm{R}}$ are defined from the covariance matrices $\mathbf{\Sigma}_{\mathrm{T}}$ and $\mathbf{\Sigma}_{\mathrm{R}}$, similarly as in the SIMO case, but at the transmitter and receiver side, respectively, $[\mathbf{G}]_{k,\ell}=x_{k,\ell}+jy_{k,\ell}$ for $k=1,\dots,N_{\mathrm{R}}$ and $\ell=1,\dots,N_{\mathrm{T}}$ where $x_{k,\ell},y_{k,\ell}\sim\mathcal{N}(0,0.5)$ are i.i.d. The area of the fluid antenna surface at the transmitter side is $W_{\mathrm{T}}=W_1^{\mathrm{T}}\lambda\times W_2^{\mathrm{T}}\lambda$ with $N_{\mathrm{T}}=N_1^{\mathrm{T}}\times N_2^{\mathrm{T}}$ evenly distributed ports. The corresponding parameters at the receiver side are defined in the same fashion. Note that vectorization is adopted to convert the 2D parameters into 1D. That is to say, the (n_1,n_2)-th port is mapped to the l-th entry, i.e., $\text{map}(n_1,n_2)=l$ for $\mathbf{\Sigma}_{\mathrm{T}}$ and $\mathbf{\Sigma}_{\mathrm{R}}$.

IV. Diversity, Multiplexing Gain and DoF

In this section, we present a few selected results that offer useful understanding of the fundamental performance of FAS in single and multiuser scenarios using the model in [29].

A. Single-user SIMO-FAS and MIMO-FAS

The outage probability of a single-user FAS was derived in closed form in [30]. At high SNR, we have [30, Theorem 5]

$$p_{\text{FAS}}=\frac{1}{\det(\mathbf{\Sigma})}\left(\frac{\Gamma}{\gamma}\right)^{-N}+o(\Gamma^{-N}), \tag{13}$$

where $\Gamma\triangleq\frac{\sigma_s^2}{\sigma_\eta^2}$ and $\det(\mathbf{\Sigma}^{-1})$ is a penalty term. The diversity order of FAS can be approximated as [30, Theorem 6]

$$d_{\text{FAS}}\approx\min(N,N'), \tag{14}$$

where N' is the numerical rank of $\mathbf{\Sigma}$ with $N\to\infty$ for a fixed W. This result reveals that increasing N over N' is not very

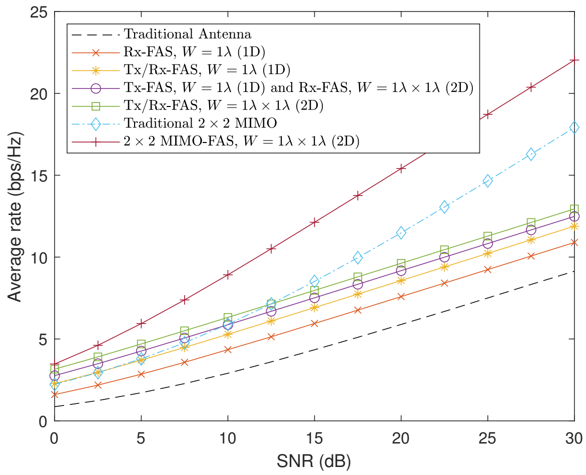

Fig. 1. Average rate of SIMO and MIMO FAS against the SNR.

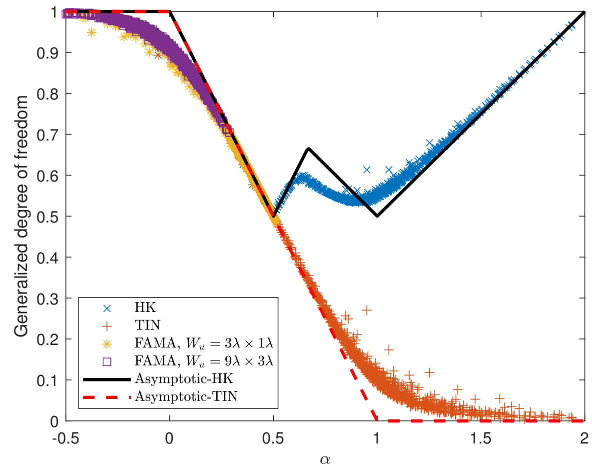

Fig. 2. gDoF of different approaches against α when $\Gamma = 30$dB.

helpful. Nevertheless, it is impossible to obtain N' analytically. Instead, [30] proposed an algorithm to compute numerically the value of N^* such that further increasing N beyond N^* will yield similar outage probability performance.

In MIMO-FAS, several ports are activated and the signals at the selected ports are combined so that the resulting received signals in vector form are expressed as

$$\tilde{\mathbf{r}} = \mathbf{W}_{\rm R}\mathbf{A}_{\rm R}\mathbf{H}\mathbf{A}_{\rm T}\mathbf{W}_{\rm T}\mathbf{s} + \mathbf{W}_{\rm R}\mathbf{A}_{\rm R}\boldsymbol{\eta}, \tag{15}$$

where $\mathbf{W}_{\rm T}$ and $\mathbf{W}_{\rm R}$ are the combining matrix, $\mathbf{A}_{\rm T}$ and $\mathbf{A}_{\rm R}$ are the port activation matrix, respectively, at the transmitter and receiver side, $\mathbf{H}$ is given by (12), $\boldsymbol{\eta}$ denotes the additive noise vector, and $\mathbf{s}$ is the information-bearing symbol vector. In [35], the joint optimization of the port activation matrices and the combining matrices has been done. It was also found that the diversity-multiplexing tradeoff (DMT) is a piecewise linear function connecting the points $(n_{\rm min}, 0)$ and

$$\left\{r, (N'_{\rm R} - r)(N'_{\rm T} - r)\right\},\ r = 0, 1, \dots, N', \tag{16}$$

where

$$N' = \arg \min_{\substack{\xi\in\mathbb{Z}\\ 0\le\xi\le n_{\rm min}-1}} \frac{(N'_{\rm R} - \xi)(N'_{\rm T} - \xi)}{n_{\rm min} - \xi} \tag{17}$$

and $n_{\rm min} = \min(n_{\rm T}, n_{\rm R})$ in which $n_{\rm T}$ and $n_{\rm R}$ are the number of activated ports at the transmitter and receiver, respectively. Additionally, $N'_{\rm T} = {\rm rank}(\boldsymbol{\Sigma}_{\rm T,red})$ where $\boldsymbol{\Sigma}_{\rm T,red}$ is a reduced covariance matrix at the transmitter side which can be obtained using [35, Theorem 7]. Same is true for $N'_{\rm R}$.

Results in Fig. 1 are provided for the average rate performance of several FASs with comparison to traditional MIMO systems for different SNR. For FAS, the number of ports is assumed to be 100. It can be observed that FAS can enhance the rate performance a lot and a 2D FAS is also more effective than the 1D counterpart. More intriguingly, incorporating FAS to MIMO brings considerable capacity gains.

B. Two-user FAMA

In the multiuser cases, the outage probability performance for fast and slow FAMA for any number of UEs was derived in [36] and [38], respectively, if the model (8) was employed. Recently, the two-user FAMA case was revisited in [41] using the model (11) and the outage probability was re-derived. For FAMA, it is important to understand the capacity scaling of the network. Assuming a fixed rate is transmitted to every UE, the multiplexing gain for FAMA can be defined as

$$m_{\rm FAMA} \triangleq (1 - p_{\rm FAMA})U \tag{18}$$

for any number of UEs, U, where $p_{\rm FAMA}$ is given by (4) or (5). If the UEs adapt their rates according to the ergodic capacity of their channels, the multiplexing gain will be defined as the scaling of the sum rate over the rate of a single-user channel.

To compliment the results in literature, here, we focus upon the two-user case and provide simulation results to compare FAMA with some popular benchmarks such as Han Kobayashi (HK) [42] and treating interference as noise (TIN). The results for the generalized DoF (gDoF),[4] i.e., the rate of a scheme over that of the AWGN channel, are illustrated in Fig. 2 against $\alpha = \frac{\log {\rm INR}}{\log {\rm SNR}}$ where INR denotes the interference-to-noise ratio. The asymptotic HK and TIN schemes are also included. According to [43], as ${\rm SNR} \to \infty$ and ${\rm INR} \to \infty$, we have

$${\rm gDoF}_{\text{asymp-HK}} = \begin{cases} 1-\alpha \text{ if } 0 \le \alpha < \frac{1}{2},\\ \alpha \text{ if } \frac{1}{2} \le \alpha < \frac{2}{3},\\ 1-\frac{\alpha}{2} \text{ if } \frac{2}{3} \le \alpha < 1,\\ \frac{\alpha}{2} \text{ if } 1 \le \alpha < 2,\\ 1 \text{ if } \alpha \ge 2, \end{cases} \tag{19}$$

and ${\rm gDoF}_{\text{asymp-TIN}} = 1 - \alpha$. Two FAMA systems in which only the UEs are equipped with a 2D fluid antenna surface are considered. One has 30×10 ports over an area of $3\lambda \times 1\lambda$ while another has 90×30 ports over an area of $9\lambda \times 3\lambda$.

The results in Fig. 2 show that the gDoFs for HK and TIN follow closely with their respective asymptotic results. The

[4]In this two-user case, the gDoF multiplied by 2 can be interpreted as the network's multiplexing gain.

results for HK suggest that if $\alpha < 0.5$, then TIN is optimal but in practice, α takes a wide range of values and HK becomes necessary to achieve the gDoF. In this regard, FAMA adds a new dimension to achieve an effective α that is small enough so that TIN is gDoF optimal, justifying why it suffices to use single-user decoding for a FAMA UE. More remarkably, the average gDoFs for TIN, HK and the two FAMA systems are, respectively, $0.146, 0.606, 0.7782$ and 0.9079.

V. Conclusion

Motivated by the rapid growth in the area of FAS, our aim was to cover the preliminaries of FAS in single and multiuser scenarios. We first reviewed the channel models used for FAS and then presented a few important results characterizing the theoretical performance of SIMO/MIMO-FAS. This letter was concluded by observing the gDoF performance of FAMA in the context of the HK scheme. The results provided theoretical evidence regarding the superiority of FAMA.

References

[1] Ericsson, "This is 5G," [Online] https://www.ericsson.com/49f1c9/assets/local/5g/documents/07052021-ericsson-this-is-5g.pdf, 2021.

[2] F. Tariq *et al.*, "A speculative study on 6G," *IEEE Wireless Commun.*, vol. 27, no. 4, pp. 118–125, Aug. 2020.

[3] NTT Docomo, Inc., "White paper: 5G evolution and 6G," Jan. 2020.

[4] Samsung, "6G: The next hyper-connected experience for all," Jul. 2020.

[5] Ericsson, "Ever-present intelligent communication," Nov. 2020.

[6] IMT-2030 Promotion Group, "White paper on 6G vision and candidate technologies," Jun. 2021.

[7] University of Surrey 5GIC Strategy Advisory Board, "6G wireless: A new strategic vision," Nov. 2020.

[8] Z. Wang *et al.*, "Extremely large-scale MIMO: Fundamentals, challenges, solutions, and future directions," [Online] arXiv:2209.12131, 2022.

[9] C. Huang, A. Zappone, G. C. Alexandropoulos, M. Debbah and C. Yuen, "Reconfigurable intelligent surfaces for energy efficiency in wireless communication," *IEEE Trans. Wireless Commun.*, vol. 18, no. 8, pp. 4157–4170, Aug. 2019.

[10] P. H. Pathak, X. Feng, P. Hu and P. Mohapatra, "Visible light communication, networking, and sensing: A survey, potential and challenges," *IEEE Commun. Sur. & Tut.*, vol. 17, no. 4, pp. 2047–2077, 2015.

[11] T. S. Rappaport *et al.*, "Wireless communications and applications above 100GHz: Opportunities and challenges for 6G and beyond," *IEEE Access*, vol. 7, pp. 78729–78757, 2019.

[12] Q. Wu and R. Zhang, "Intelligent reflecting surface enhanced wireless network via joint active and passive beamforming," *IEEE Trans. Wireless Commun.*, vol. 18, no. 11, pp. 5394–5409, Nov. 2019.

[13] R. Long, Y.-C. Liang, Y. Pei and E. G. Larsson, "Active reconfigurable intelligent surface-aided wireless communications," *IEEE Trans. Wireless Commun.*, vol. 20, no. 8, pp. 4962–4975, Aug. 2021.

[14] E. G. Larsson, O. Edfors, F. Tufvesson and T. L. Marzetta, "Massive MIMO for next generation wireless systems," *IEEE Commun. Mag.*, vol. 52, no. 2, pp. 186–195, Feb. 2014.

[15] D. A. Urquiza Villalonga, H. OdetAlla, M. J. Fernández-Getino Garca, and A. Flizikowski, "Spectral efficiency of precoded 5G-NR in single and multi-user scenarios under imperfect channel knowledge: A comprehensive guide for implementation," *Electronics*, vol. 11, no. 24, p. 4237, Dec. 2022.

[16] Y. Saito *et al.*, "Non-orthogonal multiple access (NOMA) for cellular future radio access," *IEEE Veh. Technol. Conf. Spring (VTC-Spring)*, 2-5 Jun. 2013, Dresden, Germany.

[17] K. K. Wong, K. F. Tong, Y. Shen, Y. Chen, and Y. Zhang, "Bruce Lee-inspired fluid antenna system: Six research topics and the potentials for 6G," *Frontiers in Commun. and Netw., section Wireless Commun.*, 3:853416, Mar. 2022.

[18] A. Shojaeifard *et al.*, "MIMO evolution beyond 5G through reconfigurable intelligent surfaces and fluid antenna systems," *Proc. IEEE*, vol. 110, no. 9, pp. 1244–1265, Sept. 2022.

[19] Y. Huang, L. Xing, C. Song, S. Wang and F. Elhouni, "Liquid antennas: Past, present and future," *IEEE Open J. Antennas & Propag.*, vol. 2, pp. 473–487, 2021.

[20] S. Song and R. D. Murch, "An efficient approach for optimizing frequency reconfigurable pixel antennas using genetic algorithms," *IEEE Trans. Antennas & Propag.*, vol. 62, no. 2, pp. 609–620, Feb. 2014.

[21] T. V. Hoang, V. Fusco, T. Fromenteze and O. Yurduseven, "Computational polarimetric imaging using two-dimensional dynamic metasurface apertures," *IEEE Open J. Antennas & Propag.*, vol. 2, pp. 488–497, 2021.

[22] T. Ismail and M. Dawoud, "Null steering in phased arrays by controlling the elements positions," *IEEE Trans. Antennas & Propag.*, vol. 39, no. 11, pp. 1561–1566, Nov. 1991.

[23] S. Basbug, "Design and synthesis of antenna array with movable elements along semicircular paths," *IEEE Antennas Wireless Propag. Lett.*, vol. 16, pp. 3059–3062, Oct. 2017.

[24] M. C. Johnson, S. L. Brunton, N. B. Kundtz and J. N. Kutz, "Sidelobe canceling for reconfigurable holographic metamaterial antenna," *IEEE Trans. Antennas & Propag.*, vol. 63, no. 4, pp. 1881–1886, Apr. 2015.

[25] K. K. Wong, A. Shojaeifard, K. F. Tong, and Y. Zhang, "Fluid antenna systems," *IEEE Trans. Wireless Commun.*, vol. 20, no. 3, pp. 1950–1962, Mar. 2021.

[26] P. Mukherjee, C. Psomas and I. Krikidis, "On the level crossing rate of fluid antenna systems," in Proc. *IEEE Int. Workshop Signal Process. Advances Wireless Commun. (SPAWC)*, 4-6 Jul. 2022, Oulu, Finland.

[27] L. Tlebaldiyeva, G. Nauryzbayev, S. Arzykulov, A. Eltawil, and T. Tsiftsis, "Enhancing QoS through fluid antenna systems over correlated Nakagami-m fading channels," in Proc. *IEEE Wireless Commun. & Netw. Conf. (WCNC)*, pp. 78–83, 10-13 Apr. 2022, Austin, TX, USA.

[28] L. Tlebaldiyeva, S. Arzykulov, K. M. Rabie, X. Li, and G. Nauryzbayev, "Outage performance of fluid antenna system (FAS)-aided Terahertz communication networks," in Proc. *IEEE Int. Conf. Commun. (ICC)*, 28 May-1 Jun. 2023, Rome, Italy.

[29] M. Khammassi, A. Kammoun, and M.-S. Alouini, "A new analytical approximation of the fluid antenna system channel," *IEEE Trans. Wireless Communications*, 2023.

[30] W. K. New, K. K. Wong, X. Hao, K. F. Tong, and C.-B. Chae, "Fluid antenna system: New insights on outage probability and diversity gain," *IEEE Trans. Wireless Commun.*, 2023.

[31] C. Skouroumounis and I. Krikidis, "Fluid antenna with linear MMSE channel estimation for large-scale cellular networks," *IEEE Trans. Commun.*, vol. 71, no. 2, pp. 1112–1125, Feb. 2023.

[32] L. Zhu, W. Ma, and R. Zhang, "Modeling and performance analysis for movable antenna enabled wireless communications," [Online] arXiv:2210.05325, 2022.

[33] J. O. Martínez *et al.*, "Toward liquid reconfigurable antenna arrays for wireless communications," *IEEE Commun. Mag.*, vol. 60, no. 12, pp. 145–151, Dec. 2022.

[34] W. Ma, L. Zhu, and R. Zhang, "MIMO capacity characterization for movable antenna systems," [Online] arXiv:2210.05396, 2022.

[35] W. K. New, K. K. Wong, X. Hao, K. F. Tong, C. B. Chae, "An information-theoretic characterization of MIMO-FAS: Optimization, diversity-multiplexing tradeoff and q-outage capacity," [Online] arXiv:2303.02269, 2023.

[36] K. K. Wong, and K. F. Tong, "Fluid antenna multiple access," *IEEE Trans. Wireless Commun.*, vol. 21, no. 7, pp. 4801–4815, Jul. 2022.

[37] K. K. Wong, K. F. Tong, Y. Chen, and Y. Zhang, "Fast fluid antenna multiple access enabling massive connectivity," *IEEE Commun. Lett.*, vol. 27, no. 2, pp. 711–715, Feb. 2023.

[38] K. K. Wong, D. Morales-Jimenez, K. F. Tong, and C. B. Chae, "Slow fluid antenna multiple access," *IEEE Trans. Commun.*, vol. 71, no. 5, pp. 2831–2846, May 2023.

[39] K. K. Wong, K. F. Tong, Y. Chen, Y. Zhang, and C. B. Chae, "Opportunistic fluid antenna multiple access," *IEEE Trans. Wireless Commun.*, 2023.

[40] K. K. Wong, K. F. Tong, Y. Chen and Y. Zhang, "Closed-form expressions for spatial correlation parameters for performance analysis of fluid antenna systems," *Electron. Lett.*, vol. 58, no. 11, pp. 454–457, Apr. 2022.

[41] H. Xu, K. K. Wong, W. K. New, and K. F. Tong, "On outage probability for two-user fluid antenna multiple access," in *Proc. IEEE Inter. Conf. Commun. (ICC)*, 28 May-1 Jun. 2023, Rome, Italy.

[42] T. Han and K. Kobayashi, "A new achievable rate region for the interference channel," *IEEE Trans. Inf. Theory*, vol. 27, no. 1, pp. 49–60, Jan. 1981.

[43] R. H. Etkin, D. N. C. Tse and H. Wang, "Gaussian interference channel capacity to within one bit," *IEEE Trans. Inf. Theory*, vol. 54, no. 12, pp. 5534–5562, Dec. 2008.